

IMPROVING PIXEL DIFFERENTIATION IN HOLOGRAPHIC IMAGES

JULY 11, 2021

Peter J. Christopher^{1,*}, Ralf Mouthaan¹, John P. Freeman², and Timothy D. Wilkinson¹

¹Centre of Molecular Materials, Photonics and Electronics, University of Cambridge, UK

²BAE Systems

*pjc209@cam.ac.uk

ABSTRACT

Computer generated holography (CGH) has seen a resurgence in recent years due, in part, to the rise of virtual and mixed reality systems. The majority of approaches for CGH are based on a sampled Discrete Fourier Transform (DFT) and ignore the interstitial behaviour between sampling points in the replay field. In this paper we demonstrate that neighbouring replay field pixels can interfere significantly giving the visual impression of pixel movement and increased noise. We also demonstrate that increasing the separation between target pixels reduces the interference and improves pixel quality. This phenomena is demonstrated experimentally with close agreement between model and measured result.

This work begins by introducing the concept of pixel differentiation before showing simulated models of pixel differentiation issues. Two mitigation approaches are introduced and an experimental system is then used to validate the simulation. Finally results are discussed and conclusions drawn.

Keywords Computer Generated Holography · Holographic Video · Pixel Differentiation · Time-Multiplexed

1 INTRODUCTION

Since its conception in the 1980s computer generated holography (CGH) has seen use in applications including lithography [1, 2], displays [3, 4], imaging [5, 6, 7] and optical manipulation [8, 9, 10]. CGH is enabled by the use of spatial light modulators (SLMs) that modulate either the phase or amplitude of a coherent light source in order to shape the resulting diffraction pattern. The practical constraints of SLM modulation is the primary constraint in finding suitable diffraction patterns corresponding to a target replay field.

A wide array of algorithms exist for adapting an ideal diffraction pattern to one achievable on real-world devices including simulated annealing [11], direct binary search [12] and Gerchberg-Saxton [13]. Real-world issues such as sampling, speckle and noise mean that expertise is required to use these techniques.

In this paper we introduce the issue of pixel differentiation. We start by presenting a brief background to CGH before presenting examples of pixel differentiation issues. We continue to discuss the impact of different performance factors and to present potential solution methods. Finally we discuss our findings and draw conclusions.

2 BACKGROUND

Traditional approaches to CGH are based on the use of the Discrete Fourier Transform (DFT),

$$F_{u,v} = \mathcal{F}\{f_{x,y}\} = \frac{1}{\sqrt{N_x N_y}} \sum_{x=0}^{N_x-1} \sum_{y=0}^{N_y-1} f_{xy} e^{-2\pi i \left(\frac{ux}{N_x} + \frac{vy}{N_y} \right)} \quad (1)$$

$$f_{x,y} = \mathcal{F}^{-1}\{F_{u,v}\} = \frac{1}{\sqrt{N_x N_y}} \sum_{u=0}^{N_x-1} \sum_{v=0}^{N_y-1} F_{uv} e^{2\pi i \left(\frac{ux}{N_x} + \frac{vy}{N_y} \right)} \quad (2)$$

where u and v represent the spatial frequencies and x and y represent the source coordinates. For reasons of performance, DFTs for holography are typically calculated using Fast Fourier Transforms (FFTs) calculation times of $O(N_x N_y \log N_x N_y)$ where N_x and N_y are the respective x and y resolutions [14, 15].

If the SLM aperture is modelled as an array of point impulse functions, the resultant far-field replay pattern caused can be treated as the DFT of the SLM pointwise multiplied by the illumination and pixel shape functions [16]. The coordinate systems used are shown in Figure 1 and we often refer to the projected image as the *Replay Field* and the SLM as the *Diffraction Field*.

Real-world SLMs are capable of only limited modulation, typically amplitude-only or phase-only [18, 19]. The challenge of generating an appropriate hologram then becomes that of finding function $f(x, y)$ conforming to the SLM constraints and to the relationship $F(u, v) = \mathcal{F}\{f(x, y)\}$ where \mathcal{F} represents the Fourier transform.

Additionally, it is worth noting that the target replay field values generated by the DFT are regularly sampled and the total intensity interstitially is not determined by the transform.

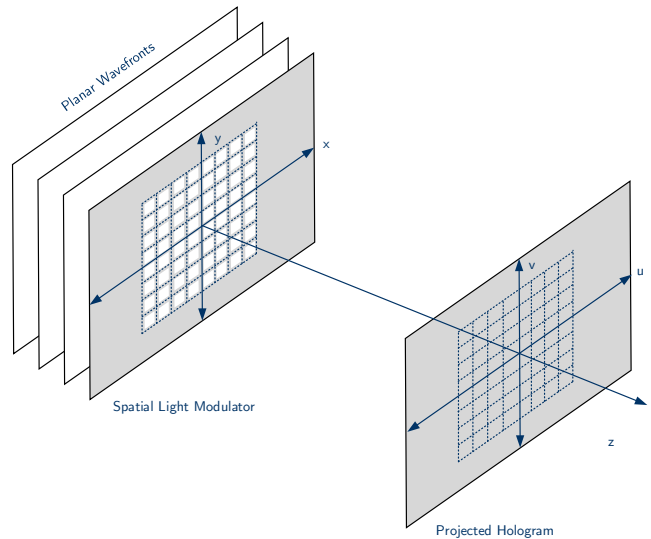


Figure 1: Hologram coordinate systems. Used with permission from: [17]

3 PIXEL DIFFERENTIATION

To introduce the problem of pixel differentiation, two separate images are considered shown in Figure 2.

Figure 2 (top, a) shows a grid of phase insensitive target pixels with a two pixel separation where the separation between pixels is taken as being the distance centre to centre. The expected replay field (b) using a DFT is shown along with a high resolution model (c). It can be seen that the shape of the replay field pixels poorly correspond to the DFT but are distinct.

The first image in Figure 2 (bottom) shows an otherwise identical case (a) where the pixels have a one pixel separation. Here the expected DFT generated replay field (b) is similar to the previous but the individual pixels are now poorly differentiated.

In both cases the hologram portions shown form the central 8×8 pixel region of a 128×128 image. The SLM pattern is taken as the superposition of gratings that form the individual pixels. This is modulated to the constraints of a phase SLM. The SLM pixels are here treated as point impulse functions.

4 THE TWO-PIXEL CASE

To better understand the behaviour here we investigate the simplest possible case, two pixels displayed by a full continuous phase SLM. The phase of the first target pixel ϕ_1 is kept constant while the phase of the second ϕ_2 is varied in the interval $(0, 2\pi]$. It is assumed that the SLM is illuminated by a perfectly collimated, top-hat profile beam.

4.1 Simultaneous

A cross section through the centres of the reconstruction against $(\phi_2 - \phi_1)$ is shown in Figure 3 for a configuration shown in Figure 4 with cross section A-A. This shows the case of SLM pixels with a 2, 1, $1/2$ pixel separation in (a), (b) and (c) respectively

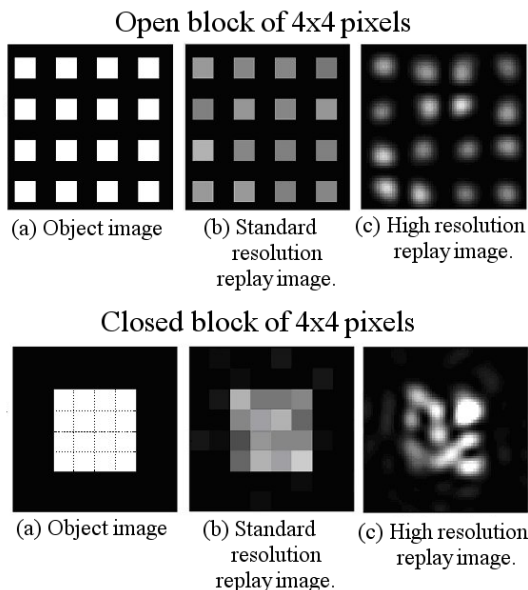


Figure 2: Pixel differentiation for a continuous phase 128×128 pixel hologram. Only the central 8×8 region of the image is shown.

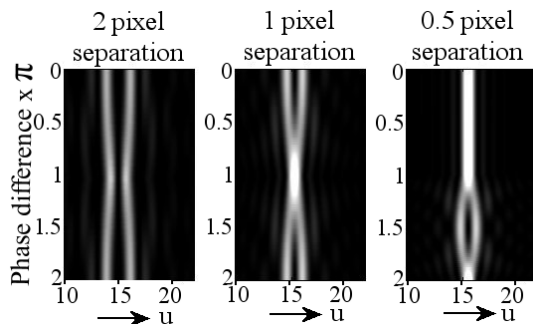


Figure 3: Section through neighbouring pixels on a 128×128 pixel hologram against difference in target phase angle between the two pixels.

and shows that the two pixels can appear to move closer together or further apart depending on phase separation.

The graph shows the distance along the u axis in the 128×128 pixel hologram used for testing with v being constant at zero. The SLM pattern is generated using superposition of constituent gratings and the cross-section is super-sampled. It will be noted that while the pixels are central in v they are offset in u for reasons discussed later.

It is worth noting also that this effect is independent of the location of the pixel pair in the target image and is only influenced by their relative phase difference and their relative spacing.

4.2 Sequential

For comparison, Figure 5 shows the case of two pixels shown alternately and the result time averaged. Here the distinction is as expected and shows distinct pixels independently of phase without the apparent pixel movement.

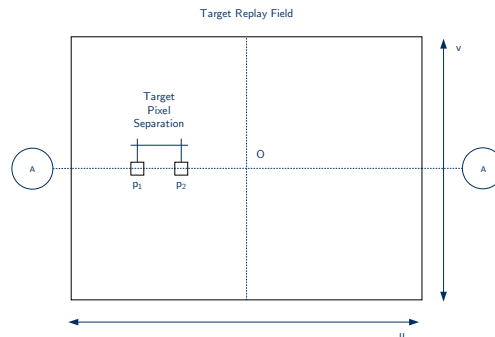


Figure 4: Configuration of replay field cross section.

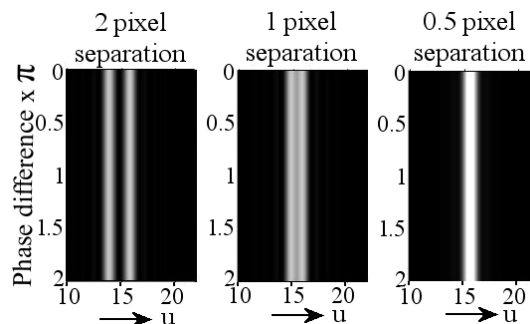


Figure 5: Time averaged section through neighbouring pixels on a 128×128 pixel hologram against difference in target phase angle between the two pixels where the pixels are shown sequentially and the impulse is integrated.

4.3 Interpretation

The difference between the simultaneous and sequential cases is stark and requires investigation. The value of a given location $H_{x,y}$ in the replay field is given as a function of target replay field values $T_{u,v}$

$$H_{x,y} = \sqrt{N_x N_y} T_{u,v} e^{2\pi i \left(\frac{ux}{N_x} + \frac{vy}{N_y} \right)} \quad (3)$$

It can be seen for a single target pixel that the required hologram is a phase grating with frequency determined by the location of the target pixel in the replay field. For two pixels, the two constituent gratings are summed. Here, however, behaviour similar to Figure 6 is observed where the two frequencies constructively and destructively interfere in a *beats*-like phenomenon. When modulated to the SLM constraints, this introduces discontinuities in the target phase profile.

This is shown further in Figure 7 where the phase holograms to generate two pixels are shown left against a close-up of the resultant image right. When the phase difference is set to π , the induced discontinuity is coincident with the hologram edge and manipulation of the phase difference between the gratings allows us to control the location of the discontinuity.

Examining Figure 8 highlights the distinction between the two contributing components.

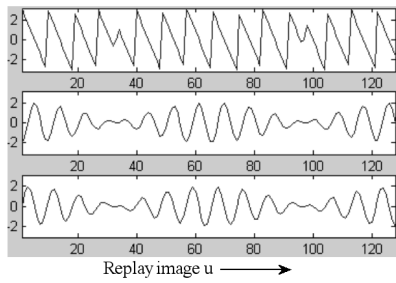


Figure 6: 1D Plot showing complex addition of 2 holograms of 2 pixels (real middle, complex bottom) resulting in the saw-tooth phase hologram with discontinuities (top).

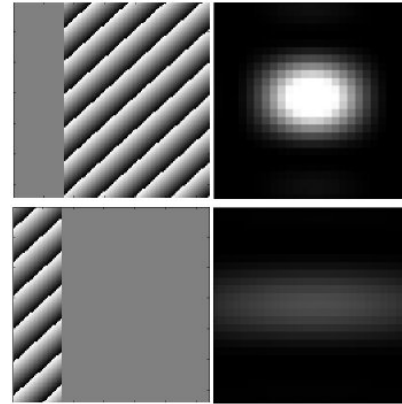


Figure 8: Separation of the two portions of Figure 7b. The uniform grey portions are taken as being zero.

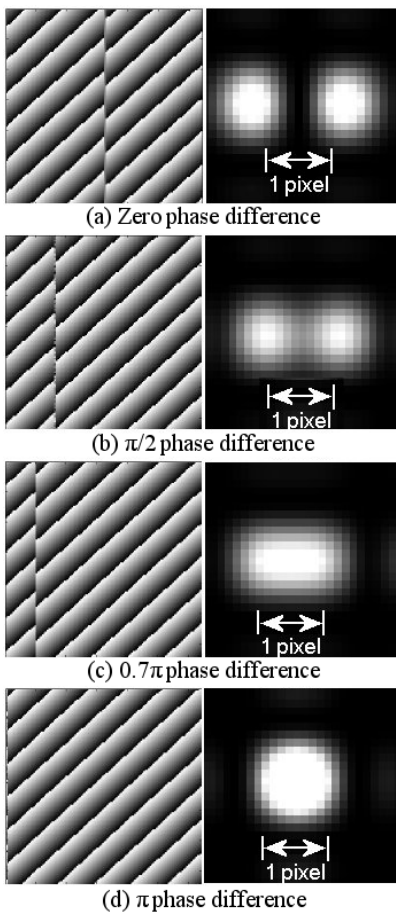


Figure 7: 128×128 phase holograms (left) used to display the replay field portions (right) that target two neighbouring pixels with a single pixel separation and the given phase difference.

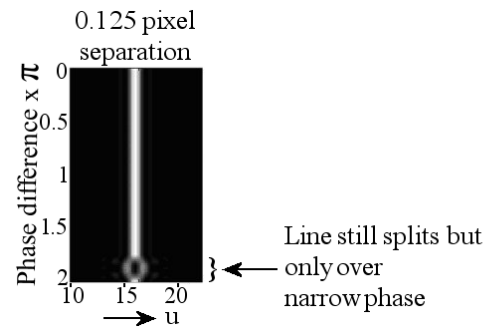


Figure 9: Section through neighbouring pixels with a 0.125 pixel spacing on a 128×128 pixel hologram against difference in target phase angle between the two pixels.

If the distance between the target pixels is changed, the periodicity of the beats phenomena is changed but still exhibits the same pixel movement behaviour and discontinuities. For example Figure 9 shows the identical case to Figure 3 but with target pixels only separated by 0.125 pixel spacing.

Additionally, this two pixel case is independent of the resolution of the SLM. For example, Figure 3 is reproduced in Figure 10 but for the case of a 1024×1024 hologram.

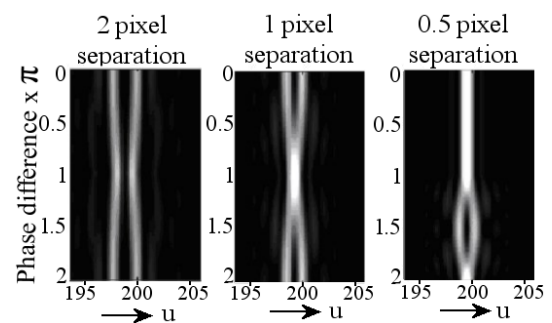


Figure 10: Section through neighbouring pixels on a 128×128 pixel hologram against difference in target phase angle between the two pixels.

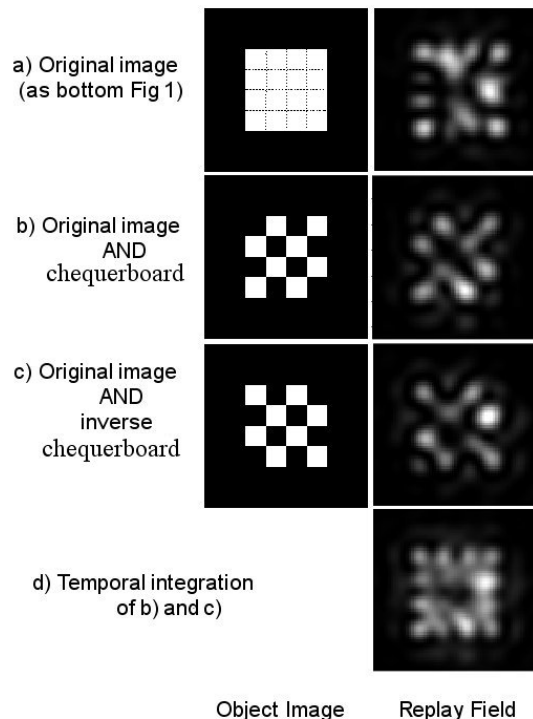


Figure 11: Temporally alternating pixels to prevent coherent interference from neighbouring pixels and so improve image.

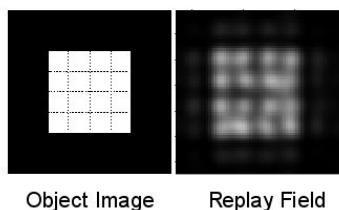


Figure 12: Temporal integration of extra alternating frames so to prevent interference from diagonals as well.

5 APPLICATION

5.1 Frame Averaging

The results in Section 4 and in particular Figure 5 suggest a means of mitigation of these effects, that of sequential pixel display.

If we are using a sufficiently fast SLM, we can rely on the time averaging effects of the human eye to integrate multiple sub-frames. This is a technique that has been used extensively in previous holographic video research [20].

By separating the pixels so that horizontal neighbours are shown independently, we can reduce the amount of interdependence between neighbouring pixels. For example Figure 11a shows the case shown previously in Figure 2. This target image is then split into two portions in (b) and (c), holograms generated for the portions and then the results shown in (d). Here it will be seen that the image quality observed is much higher.

This approach is taken further in Figure 12 where diagonally neighbouring pixels are also shown independently leading to the

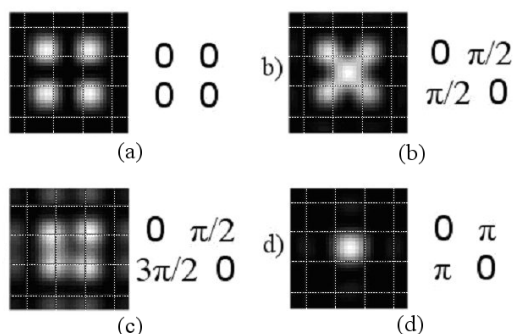


Figure 13: Pixel differentiation for a 2×2 square of pixels with defined phase difference embedded in a continuous phase 128×128 pixel hologram. A single pixel grid is superimposed for reference.

sum of four independent sub-frames. Here the image quality is greatly improved with all pixels being clearly distinct at the expense of using 4 independent sub-frames.

5.2 Single Frame Manipulation

For applications where it is impractical to show sequential sub-frames, controlling phase relationships between pixels allows for improvements in pixel differentiation. This is in contrast to the random phase approach used earlier. As suggested in Figure 3, neighbouring pixels have the best independence with a pixel separation of either $\pi/2$ or $3\pi/2$.

Figure 13 shows the case of a 2×2 block of neighbouring pixels with defined phase differences. The worst case of repelling is shown in (a) with the worst case of attraction in (d). The case in (b) shows the case of $\pi/2$ neighbouring pixel separation but with similar diagonals and (c) shows a similar case but with diagonals separated by π . Here it can be seen that the defined phase of (c) leads to the best behaviour in pixel location but still involves significant error.

We can extend this to the 4×4 block shown in Figure 2 and with judicious tiling can get the behaviour shown in Figure 14. Again, while pixel differentiation is not perfect, it is significantly improved from Figure 2.

6 THE EFFECT OF QUANTISATION LEVELS

The modeling shown until now has been using a continuous phase SLM. For real-world applications it is likely that these techniques will be used on multi-level or binary devices. If we ignore the effects of higher orders, we can reproduce the results of Figure 3 for a binary phase SLM to give Figure 15. As before, the holograms are generated by superimposing constituent gratings and constraining the result to the SLM achievable states. Again, the pixels appear to move relative to each other.

7 EXPERIMENTAL VERIFICATION

In order to confirm the modelling done, we showed the holograms generated for Figure 15 on a binary Electrically Addressable Spatial Light Modulator (EASLM) in a configuration shown

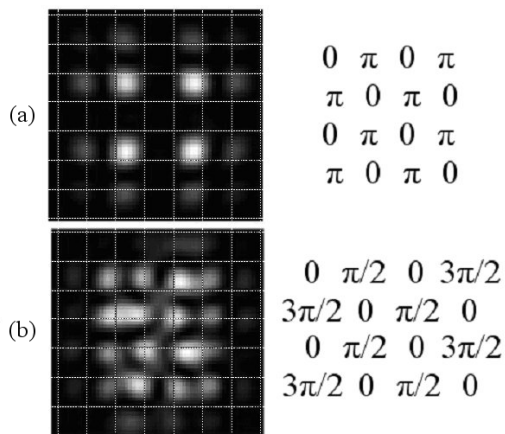


Figure 14: Pixel differentiation for a 4×4 square of pixels with defined phase difference embedded in a continuous phase 128×128 pixel hologram. A single pixel grid is superimposed for reference.

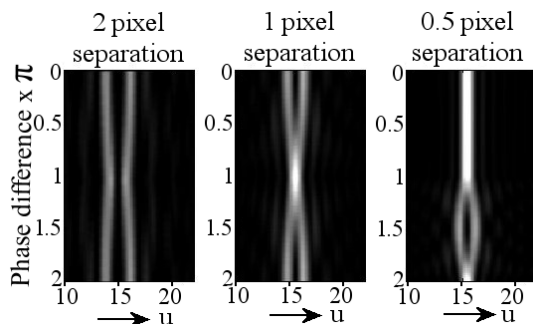


Figure 15: Pixel differentiation for a 4×4 square of pixels with defined phase difference embedded in a continuous phase 128×128 pixel hologram. A single pixel grid is superimposed for reference.

in Figure 16. The EASLM available was a CRLOpto (now Forth Dimension) binary device with 1280×1024 pixels and $13.6\mu\text{m}$ pixel pitch. We showed the binary holograms on the central 128×128 pixel region and confirmed flatness using a Fabry-Perot interferometer. The hologram was displayed using a $2f$ system with a 150mm focal length doublet focussing the replay image onto a CCD camera. The row of pixels from the camera, passing through the replay image of both dots was then extracted and used to build the plot.

It will be noticed that there is a high degree of similarity between the theoretical model and the experimental results with the addition of some additional noise.

8 SUMMARY AND RECOMMENDATIONS

This paper has presented the observation of the interplay between neighbouring pixels in CGH. Whereas the replay field sampling is equivalent to the DFT of a given SLM aperture function, the interstitial behaviour can vary significantly. By summing the individual SLM pixel contributions for interstitial

points we can get a higher resolution understanding of individual replay field pixels.

Our main observation in this work is that neighbouring pixels appear to repel or attract each other depending on their relative phase differences. We have presented a mathematical argument that this is due to a form of beating behaviour between the individual pixel contributions.

This effect was seen to be independent of the location of the pixel and was only influenced by their relative phase difference and their relative spacing. Additionally, the effect was independent of the image resolution.

In the light of this we suggested two mitigation techniques. The first involved time-averaging of neighbouring pixels. Doing this allowed for much clearer pixel differentiation at the cost of requiring additional sub-frames. The second involved replacing the phase randomisation step with a defined phase difference between neighbouring pixels.

We then extended our results to the case of a binary phase SLM demonstrating similar results before introducing an experimental system. This confirmed the pixel movement observed.

Often when comparing an experimental holographic image with a theoretically expected result the observed noise is assumed to be attributable to a variety of sources including: speckle, non-flatness of the SLM, beam shape and atmospheric effects. On the basis of this work, we suggest that even in a theoretically perfect system, the sampled replay field can be a poor indicator of the actual image displayed.

The effects we have shown here of pixel movement is not observable in a sampled replay field and that interstitial behaviour in the replay field should be considered when discussing algorithms. It is suggested that some of the experimental noise observed in real-world systems may be attributed to hologram generation approach used rather than imperfections in the physical system.

While we have discussed here a simple example of apparent pixel movement, we are aware that many other complex effects are likely and further research is recommended.

9 CONCLUSION

In this work we have presented a theoretical investigation of interstitial noise in hologram generation and have highlighted one particular area. That of pixel differentiation. We have examined this phenomena in detail discussing variables that influence behaviour. Informed by this we have presented two techniques for mitigation and given recommendations for future study.

Acknowledgements

This paper is based on an unpublished work "Resolution in the Replay Field of a Holographically Generated Video Image" by JPF and TDW. PJC and RM are responsible for updating and extending this paper and have done so with permission.

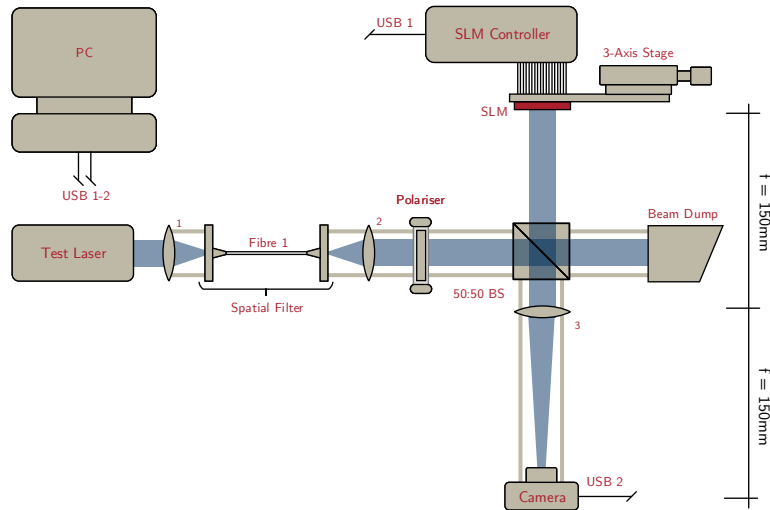


Figure 16: Experimental configuration.

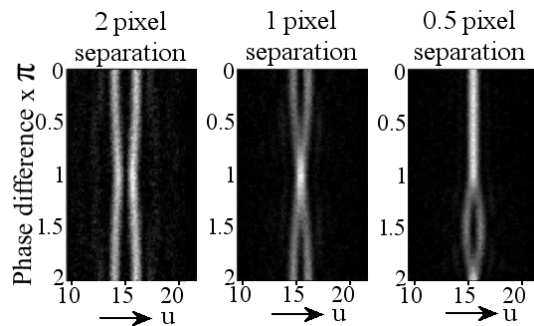


Figure 17: Experimental confirmation of pixel differentiation results.

Funding

PJC and RM would like to thank the Engineering and Physical Sciences Research Council (EP/L016567/1 and EP/L015455/1) for funding through the period of this research.

JPF would like to thank BAE Systems for sponsorship and support.

Disclosures

The authors declare no conflicts of interest.

REFERENCES

- [1] A. J. Turberfield, M. Campbell, D. N. Sharp, *et al.*, “Fabrication of photonic crystals for the visible spectrum by holographic lithography,” *Nature* **404**(6773), 53–56 (2000).
- [2] A. Purvis, J. J. Toriz-Garcia, J. J. Cowling, *et al.*, “Holographic lithography,” in *Imaging and Applied Optics 2014*, *Imaging and Applied Optics 2014*, DW1B.1, Optical Society of America (2014).
- [3] A. Maimone, A. Georgiou, and J. S. Kollin, “Holographic near-eye displays for virtual and augmented reality,” *ACM Transactions on Graphics* **36**(4), 1–16 (2017).
- [4] S. Yamada, T. Kakue, T. Shimobaba, *et al.*, “Interactive Holographic Display Based on Finger Gestures,” *Scientific Reports* **8**(1), 1–7 (2018).
- [5] J. Svoboda, M. Škereň, M. Květoň, *et al.*, “Holographic 3d imaging – methods and applications,” *Journal of Physics: Conference Series* **415**, 012051 (2013).
- [6] Y. Frauel, T. J. Naughton, O. Matoba, *et al.*, “Three-dimensional imaging and processing using computational holographic imaging,” *Proceedings of the IEEE* **94**, 636–653 (2006).
- [7] D. M. Sheen, D. L. McMakin, and T. E. Hall, “Three-dimensional millimeter-wave imaging for concealed weapon detection,” *IEEE Transactions on Microwave Theory and Techniques* **49**(9), 1581–1592 (2001).
- [8] D. G. Grier and Y. Roichman, “Holographic optical trapping,” *Appl. Opt.* **45**, 880–887 (2006).
- [9] H. Melville, D. Milne, G. Spalding, *et al.*, “Optical trapping of three-dimensional structures using dynamic holograms,” *Optical Express* **11**(26), 3562–3567 (2003).
- [10] J. A. Grieve, A. Ulcinas, S. Subramanian, *et al.*, “Hands-on with optical tweezers: a multitouch interface for holographic optical trapping,” *Optics Express* **17**(5), 3595 (2009).
- [11] S. Kirkpatrick, C. D. Gelatt, M. P. Vecchi, *et al.*, “Optimization by simulated annealing,” *science* **220**(4598), 671–680 (1983).
- [12] D. W. S. Brian K. Jennison, Jan P. Allebach, “Iterative approaches to computer-generated holography,” *Optical Engineering* **28**(6), 629 – 637 – 9 (1989).
- [13] R. W. Gerchberg and W. O. Saxton, “A practical algorithm for the determination of phase from image and diffraction plane pictures,” *Optik* **35**(2), 237–246 (1972).

- [14] J. Carpenter, “Graphics processing unit–accelerated holography by simulated annealing,” *Optical Engineering* **49**(9), 095801 (2010).
- [15] M. Frigo and S. G. Johnson, “The design and implementation of fftw3,” *Proceedings of the IEEE* **93**(2), 216–231 (2005).
- [16] J. W. Goodman, *Introduction to Fourier Optics, Third Edition*, Roberts and Company Publishers (2004).
- [17] P. J. Christopher, J. D. Lake, D. Dong, *et al.*, “Improving holographic search algorithms using sorted pixel selection,” *Journal of the Optical Society of America A* **36**, 1456–1462 (2019).
- [18] Y. Huang, E. Liao, R. Chen, *et al.*, “Liquid-Crystal-on-Silicon for Augmented Reality Displays,” *Applied Sciences* **8**(12), 1–17 (2018).
- [19] J. L. de Bougrenet de la Tocnaye and L. Dupont, “Complex amplitude modulation by use of liquid-crystal spatial light modulators,” *Applied Optics* **36**(8), 1730 (1997).
- [20] P. J. Christopher, R. Mouthaan, V. Bheemireddy, *et al.*, “Improving performance of single-pass real-time holographic projection,” *Optics Communications* **457**, 124666 (2020).